Phase behaviour and solution properties of sulphobetaine polymers

D. N. Schulz, D. G. Peiffer, P. K. Agarwal, J. Larabee, J. J. Kaladas, L. Soni, B. Handwerker and R. T. Garner

Corporate Research Science Labs., Exxon Research and Engineering Co., Annandale, NJ 08801, USA

(Received 10 January 1986; revised 5 May 1986)

Aqueous polyelectrolytes have been extensively studied and comprehensively described in numerous books and reviews. In contrast, systematic investigations of aqueous polyzwitterions are few. This paper describes the detailed phase behaviour and solution properties of a homopolymer based upon a recently available sulphobetaine monomer, *N*-(3-sulphopropyl)-*N*-methacrylooxyethyl-*N*,*N*-dimethyl ammonium betaine (SPE). In addition, such properties are probed at the molecular level by static and dynamic light scattering, as well as laser Raman spectroscopy. Poly[*N*-(3-sulphopropyl)-*N*-methacrylooxyethyl-*N*,*N*-dimethyl ammonium betaine], P(SPE), of 4.35×10^5 M_w shows remarkable phase behaviour. It exhibits both an upper critical solution temperature (*UCST*) and an 'apparent inverted' lower critical solution temperature (*LCST*), i.e. a 1-phase region flanked by two 2-phase regions. Moreover, the *UCST* occurs at an order of magnitude lower polymer concentration than predicted by theory or demonstrated by experiment with conventional polymers. The aqueous solubility of (SPE) depends upon polymer molecular weight, as well as the concentration and structure of added salts. 'Soft' salt anions and cations are more effective solubilizers than 'hard' anions and cations. Furthermore, solutions of P(SPE) display 'antipolyelectrolyte behaviour', i.e. viscosities which increase with increasing salt concentrations. Static light scattering experiments indicate that the solvent quality for P(SPE) increases with increasing salt concentration. Dynamic light scattering measurements show that the polymer diffusion coefficients decrease and the chain dimensions increase with increasing salt concentrations. Moreover, laser Raman spectroscopy indicates that the local environment around the zwitterion functionalities is also modified by changes in salt concentration. Based upon such molecular level probes, models have been proposed to account for the P(SPE) phase behaviour and solubility. Thus, P(SPE) is depicted as a collapsed coil in water because of intra-group and intra-chain associations. The unusual phase behaviour of P(SPE) in water is rationalized in terms of a shift from intra- to interinteractions. In turn, NaCl breaks up the intra-associations and promotes polymer solubility.

(Keywords: poly(sulphobetaines); phase behaviour; antipolyelectrolytes; solution properties)

INTRODUCTION

Aqueous polyelectrolytes of all types have been extensively studied and comprehensively described in numerous books and reviews[1-12]. In contrast, systematic examinations of aqueous polyzwitterions are few. For example, aside from the initial communication of Hart[13] and the more recent in-depth studies of Salamone[14] and Galin[15], there is very little in the open literature on sulphobetaine polymers, i.e. polyzwitterions of the type

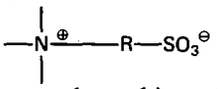

The dearth of research on this topic is surprising since sulphobetaines are phenomenologically interesting by virtue of their 'antipolyelectrolyte' solution behaviour: e.g. enhanced viscosities in salt solutions. Furthermore, in the recent past, some new sulphobetaine monomers such as SPE (**I**), have become commercially available[16].

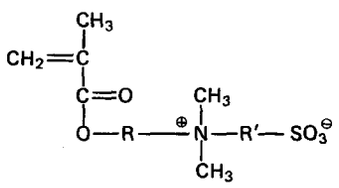

(I)
(SPE)

Thus, sulphobetaine polymers are both scientifically rich and ripe for further study. This paper describes the detailed phase behaviour and solution properties of homopolymers of the sulphobetaine monomer, SPE. Besides uncovering new aspects of the phase behaviour of sulphobetaine polymers, we have probed such polymers at the molecular level with static (LALLS) and dynamic (QELS) light scattering, as well as laser Raman spectroscopy. In addition, we have proposed models to describe their properties.

EXPERIMENTAL

Typical preparation of P(SPE)

A one litre reaction flask was fitted with a thermometer, an air stirrer, a condenser and a nitrogen inlet tube. A 500 g quantity of distilled H_2O was purged for one hour under a subsurface nitrogen purge. The nitrogen inlet tube was then raised above the surface and 71.2 g of the SPE monomer, *N*-(3-sulphopropyl)-*N*-methacrylo-oxyethyl-*N*,*N*-dimethyl ammonium betaine (Rasching Co.) was dissolved in the purged water. Subsequently, 1.2 g of $(NH_4)_2S_2O_4$ initiator was charged. The batch was stirred at 50°C under a nitrogen blanket for 18 h. The batch was subsequently cooled and precipitated in methanol, washed with acetone, isolated and dried at 30°C under vacuum. Conversion was 80%. The structure

0032-3861/86/111734$03.00

of the polymer was confirmed by elemental analyses and ^{1}H n.m.r. spectroscopy (below), as well as laser Raman spectroscopy (see *Results and Discussion* section).

P(SPE) (Theory): 5.01% N; 11.48% S

P(SPE) (Actual): 4.90% N; 11.51% S

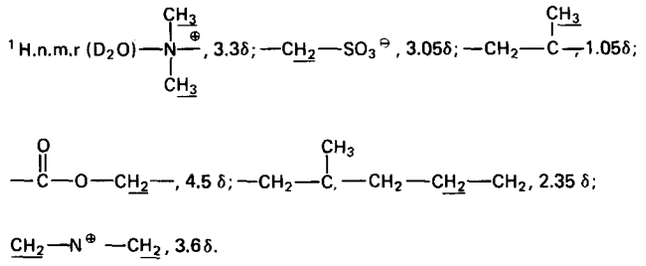

Phase behaviour measurements

Cloud points of diluted P(SPE) solutions were determined in water and salt solutions. Stock solutions of polymer were diluted to appropriate concentrations in weight %, which approximates volume % for aqueous systems.

Each sample was stirred magnetically for a period of 10 min prior to the cloud point determination. A sample of polymer solution (*ca.* 4 ml) was poured into a test tube, and a thermometer placed directly into the tube. Solutions, which were clear at room temperature following stirring, were cooled by means of an ice bath. The cloud transition point was taken as the temperature at which the solution first turned cloudy. The cloudy solution was then heated in a water bath; the cloudy to clear point was recorded as the temperature at which the solution just turned transparent. In cases in which the solutions were cloudy at room temperature following stirring, the solutions were heated well above the transition point before they were immersed in an ice bath. The transition temperature was noted when the solution first turned cloudy. Unless otherwise indicated, the results described herein are for the clear to cloudy transition. Generally, the two cloud point methods have agreed within ± 2°C for salt solutions and within ± 4°C for water solutions. These deviations are likely caused by polydispersity effects.

Low-angle light scattering measurements

Molecular weight ($\bar{M}_w$) and second virial coefficient (A_2) measurements were made on a KMX-6 fixed low-angle light scattering spectrometer (LALLS) at 25°C. Molecular weight measurements were made in 2% w/w NaCl. The refractive index increment (dn/dc in 2% NaCl = 0.157) for P(SPE) was determined on a KMX-16 differential refractometer at 25°C.

Quasielastic light-scattering (QELS) measurements

The polymer solutions were prepared in stoppered volumetric flasks utilizing conventional magnetic stirrers for agitation. The polymer was weighed into the flask to an accuracy of 0.002 g. The solutions used in the QELS measurements were carefully filtered prior to placement into the light scattering apparatus.

The quasielastic light scattefring instrument used in these experiments was the Brookhaven Instruments Model BI-2030 with a digital correlator. The He–Ne laser used was a Spectra Physics Model 1248 operating at 35 mW power (6328 Å). All QELS measurements were performed at 40.2°C in the dilute solution regime, i.e. polymer concentration was 1000 ppm.

The hydrodynamic diameter of the betaine homopolymer was measured utilizing the quasielastic light scattering (QELS) technique. QELS is a correlation function measurement of the temporal intensity fluctuation, $I(t)$, which is

$$c(\tau) \equiv \langle I(t)I(t+\tau)\rangle / \langle I(t)\rangle^2$$

where τ is a delay time. In more physical terms, such light scattering can be observed where the incident light is modulated during scattering by the Doppler effect arising on particles which move randomly via Brownian motion. Under this circumstance, the temporal fluctuations are governed by the molecular diffusion process given by the correlation function

$$c(\tau) = Ae^{-2Dq^2\tau} + B$$

where D is the translational diffusion coefficient, q is the scattering vector, and A and B are constants whose value depends on the scattering geometry. From the value of D, as determined by the time dependency of the fluctuation τ, the mean hydrodynamic diameter is calculated by using the Einstein–Stokes relationship, i.e.

$$D_H = 2\bar{R}_H = \frac{kT}{3\pi\eta\bar{D}}$$

where k is the Boltzmann constant, T is absolute temperature, and η is the solvent viscosity. Since $\bar{D}$ is an average translation diffusion coefficient, D_H or $2\bar{R}_H$ represents the average hydrodynamic diameter of all polymer molecules present in the solution. Even though the polymer molecules used in this study are not monodispersed, a single decay exponential fits the correlation function quite well. Nevertheless, it is appropriate in such measurements still to regard $D_H(2\bar{R}_H)$ and $\bar{D}$ as averages over a large number of species.

Laser Raman measurements

Raman spectra were recorded on a system consisting of a Spex 1403 double monochromator, Datamate data system, Spectra Physics model 171-18 Ar ion laser, RCA C31034 photomultiplier tube with photon counting electronics and Newport optical table. Spectra were recorded at a resolution of 4 cm^{-1} with 2 s photon counting. As many as 20 sequential scans were added to improve the signal to noise ratio. All data were collected using real time Raman difference spectroscopy. This technique[17] allows for the determination of very small (0.1 cm^{-1}) shifts in Raman bands, even if the width at half height is much larger than the shift. The difference apparatus, which is available from Spex, consists of a split liquid spinning cell and a sample rotator which is linked to the data system so that the Raman scattering from each side of the cell goes into separate data files. Since data from both sides of the sample cell are collected at the same grating position, scanning errors are eliminated.

RESULTS AND DISCUSSION

Betaines are special classes of zwitterions which have isolated, nonadjacent cationic and anionic sites, as well as

not possessing a hydrogen atom bonded to the cationic site. Additionally, sulphobetaines prepared by condensation of amines with propane or butane sultone possess no other counterions (equation (1)).

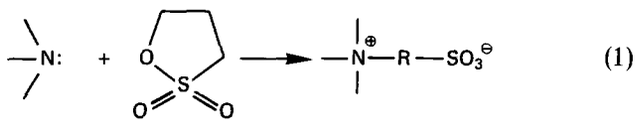

(1)

Phase behaviour of P(SPE)

Previous workers[13–15] have found that sulphobetaine polymers show enhanced solubilities in salt solutions compared with purely aqueous media. However, none of these workers determined the entire phase diagrams for such materials. Instead, they merely determined the minimum amount of salt required to effect polymer dissolution at a fixed polymer concentration. Consequently, we felt it would be worthwhile to map out the entire phase boundaries for P(SPE) in water and various salt solutions over a relatively broad range of polymer concentrations. In so doing, we have discovered some remarkable phase behaviour for these materials.

Conventional polymers customarily show an upper critical solution temperature (*UCST*), a lower critical solution temperature (*LCST*) *or* a closed loop of insolubility. In contrast, P(SPE) of 4.35×10^5 $\bar{M}_w$ in H_2O shows *both* an *UCST* (33°C) and an 'apparent inverted' *LCST* (16°C) (*Figure 1*). Thus, if one traverses the phase diagram at 25°C, for example, one observes solubility (1-phase region) $\leqslant 0.03\%$, insolubility (2-phase region) from 0.03% to 0.8%, solubility again between 0.8–25%, and finally insolubility at $> 25\%$ polymer.

The most unusual portion of this phase map is the 1-phase region flanked by two 2-phase regions. In this part of the phase space, one paradoxically adds additional polymer to dissolve an insoluble material. This 'inverted *LCST*' occurs in the neighbourhood of the overlap concentration, C^*. As will be described later, we believe that this solubility behaviour results from a shift from insolubility caused by intramolecular associations (by ionic and H-bonding interactions) to solubility induced by intermolecular interactions. The latter interactions surprisingly facilitate solubilization of the chains at low levels. At higher levels, intermolecular interactions become so dominant that precipitation again occurs. Of course, one cannot rule out polydispersity effects

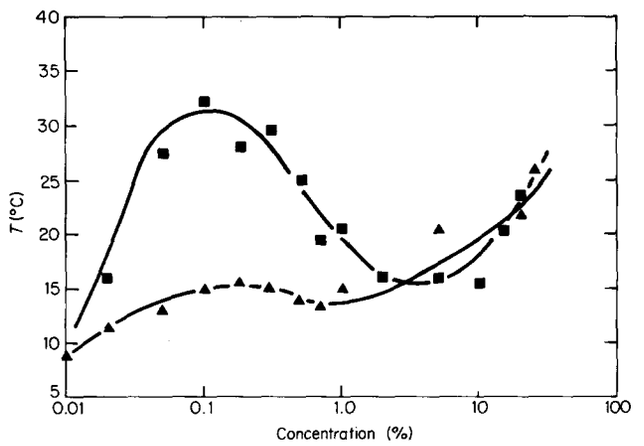

Figure 1 Effect of polymer concentration and salt on P(SPE) phase behaviour. Polymer $\bar{M}_w = 4.35 \times 10^5$; ■, H_2O; ▲, 0.3% NaCl (0.51 M)

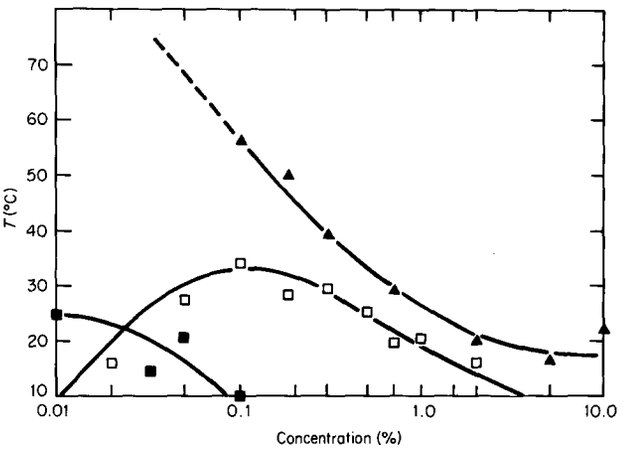

Figure 2 Effect of polymer molecular weight on P(SPE) phase behaviour. ▲, $\bar{M}_w = 7.1 \times 10^5$; □, $\bar{M}_w = 4.3 \times 10^5$; ■, $\bar{M}_w = 1.5 \times 10^5$

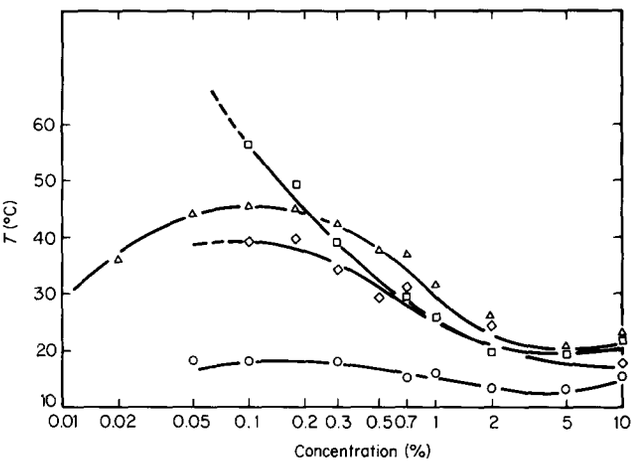

Figure 3 Effect of salt concentration on P(SPE), $M_w = 7.1 \times 10^5$, phase behaviour. □, H_2O; △, 0.05% NaCl (0.085 M); ◇, 0.1% NaCl (0.17 M); ○, 0.3% (0.51 M)

as contributing somewhat to the unusual shape of the phase diagram[18–21]. The salt diagram for P(SPE) (*Figure 1*) also exhibits an unusual shape, but the magnitude of the effect is less dramatic than for the case of P(SPE) in H_2O.

The critical temperatures of conventional polymers normally increase with increasing molecular weight[22]. This is also the case for P(SPE) in H_2O (*Figure 2*). The *UCST* for P(SPE) goes from ~ 25°C to > 55°C as the molecular weight goes from 1.5–7.1×10^5. Unlike the critical temperature, the critical composition for P(SPE) in water is not normal. The critical composition occurs at an order of magnitude lower concentration than predicted by theory or demonstrated by experiment with conventional hydrocarbon nonfunctional polymers, e.g. polyisobutylene or polystyrene of similar chain lengths[22]. We believe that a strongly intramolecularly associated polymer would tend to phase out of solution at a lower concentration than a conventional polymer because such interactions would tend to enhance collapse of the polymer coil.

Salt lowers the *UCST* of P(SPE), as seen in *Figure 1*. Moreover, the degree of diminution of the *UCST* is a function of salt concentration and the anion and cation structures of the salts. For example, the greater the salt concentration, the greater is the extent of the 1-phase region (*Figure 3*).

The effect of salt anion structure on P(SPE) phase behaviour is shown in *Figures 4* and *5*. The orders of

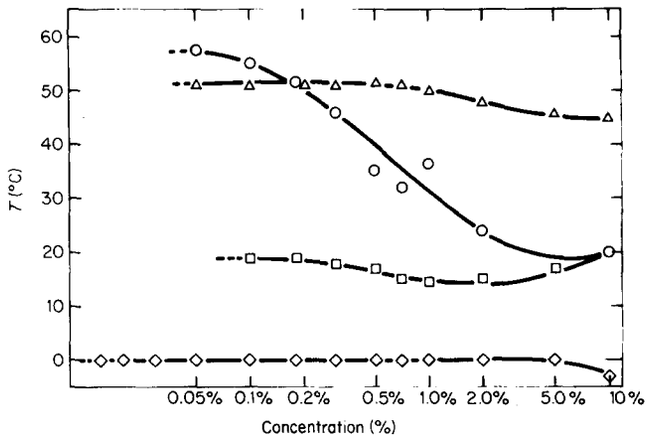

Figure 4 Effect of salt anion structure on P(SPE), $M_w = 7.2 \times 10^5$, phase behaviour: ○, H_2O; △, 0.05 M Na_2CO_3; □, 0.5 M NaCl; ◇, 0.05 M NaSCN

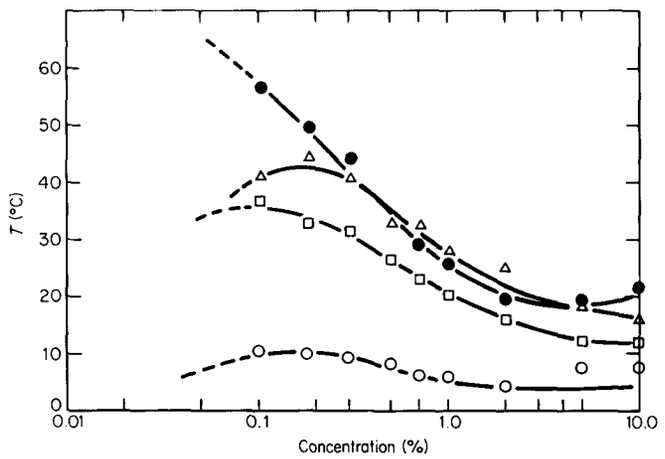

Figure 5 Effect of salt anion structure on P(SPE), $\bar{M}_w = 7.1 \times 10^5$, phase behaviour. ●, H_2O; △, NaCl (0.05%); □, NaBr (0.05%); ○, NaI (0.05%)

solubilizing power for a fixed $Na^{\oplus}$ cation structure are:

$$SCN^{\ominus} > Cl^{\ominus} > CO_3^{\ominus} \qquad I^{\ominus} > Br^{\ominus} > Cl^{\ominus}$$

These sequences follow the Hofmeister 'lyotropic series'[23] for ranking the ability of electrolytes to 'salt in' or 'salt out' polymers from aqueous solutions. The $SCN^{\ominus}$ ion is known as a 'salting in' anion; the $Cl^{\ominus}$ ion is an 'intermediate' anion; the $CO_3^{\ominus}$ is a 'salting out' anion[23-25].

The order of anion structure also follows the 'hard–soft' acid–base theory[26]. The relatively 'soft' ammonium cation prefers the 'softer' salt anions of $I^{\ominus}$ and $SCN^{\ominus}$. The anion ranking also confirms the trends reported by Galin[15] and Salamone[14] for other sulphobetaine polymers.

Whereas there has been some agreement about the order of anion type toward solubilizing sulphobetaine polymers, there have been differences in the order of cation ranking[14,15]. *Figure 6* shows the order of cation ranking for monovalent cations at salt concentrations (0.024 M) below that necessary to neutralize all the charges of the zwitterion. Clearly, the order among the alkali metals ($Li^{\oplus}$, $Na^{\oplus}$, $K^{\oplus}$) depends upon where on the phase map the comparison is made. Such a variation may account for the discrepancies in the cation order of previous studies, which depended upon single concentration cloud-point measurements. Nevertheless, the differences between the alkali metal cations is small because these are all 'hard' acid centres. The addition of softer cations, such as $Ag^{\oplus}$, is clearly more effective at solubilizing the soft anion of P(SPE), i.e. the $-SO_3^{\ominus}$ group.

The effect of $Ag^{\oplus}$ is particularly notable because the salt used is $AgNO_3$, where the $NO_3^{\ominus}$ is a 'hard' anion. At salt concentrations above that necessary to 'neutralize' all of the zwitterion charges (0.5 M), the order of cation solubilization power for monovalent cation becomes

$$Ag^{\oplus} > N^{\oplus}(n\text{-}C_4H_9)_4 \gg K^{\oplus} \approx Na^{\oplus} > Li^{\oplus}$$

where again the 'softer' cations ($Ag^{\oplus}$, $N^{\oplus}(n\text{-}C_4H_9)_4$) are more effective than the 'harder' alkali metal cations (*Figure 7*).

The cation order of bivalent alkaline earth cations was found to be:

$$Ba^{\oplus\oplus} \approx Ca^{\oplus\oplus} > Mg^{\oplus\oplus}$$

as shown in *Figure 8*. This order roughly follows ionic radii trends. However, one does not expect large differences between these cations because they are all 'hard' cations.

The H-bond breakers like urea are also capable of reducing the *UCST* of P(SPE) (*Figure 9*). However, the power of urea to solubilize the P(SPE) is much less than

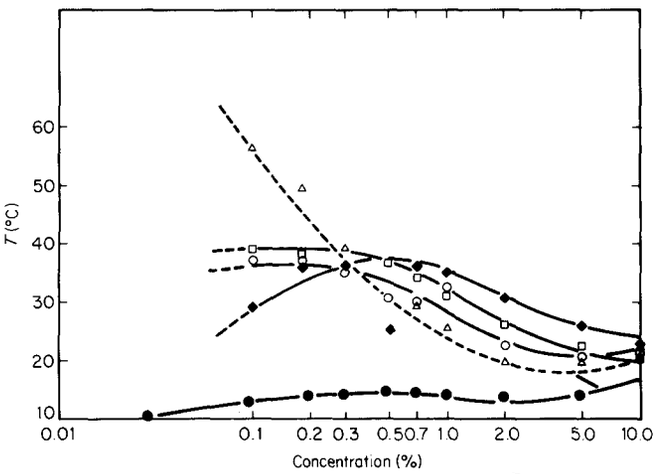

Figure 6 Effect of salt cation structure on P(SPE), $\bar{M}_w = 7.1 \times 10^5$, phase behaviour. △, H_2O; ◆, 0.024 M LiCl; ○, 0.024 M NaCl; □, 0.024 M KCl; ●, 0.025 M $AgNO_3$

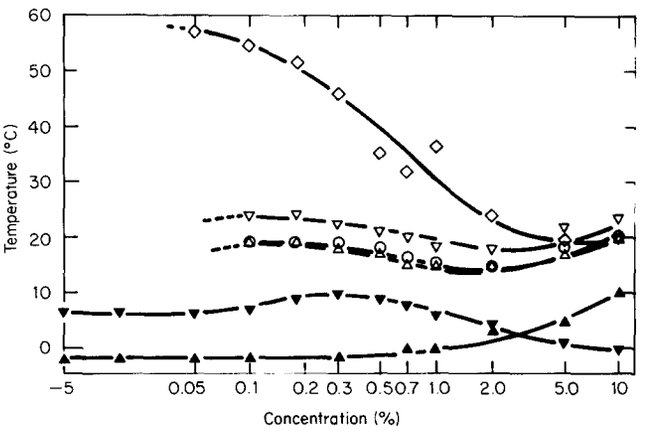

Figure 7 Effect of salt cation structure on P(SPE), $\bar{M}_w = 7.2 \times 10^5$, phase behaviour. □, H_2O; ▽, 0.05 M LiCl; △, 0.05 M NaCl; ○, 0.05 M KCl; ▼, 0.05 M $N^+(C_4H_9)_4Cl$; ▲, 0.05 M $AgNO_3$ (freezes below 1.0% polymer)

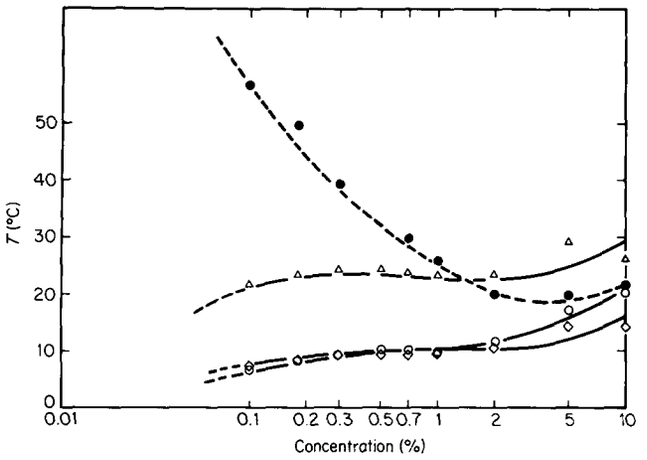

Figure 8 Effect of salt cation structure on P(SPE), $\bar{M}_w = 7.1 \times 10^5$, phase behaviour. ●, H_2O; △, 0.095 M $MgCl_2$; □, 0.095 M $CaCl_2$; ○, 0.095 M $BaCl_2$

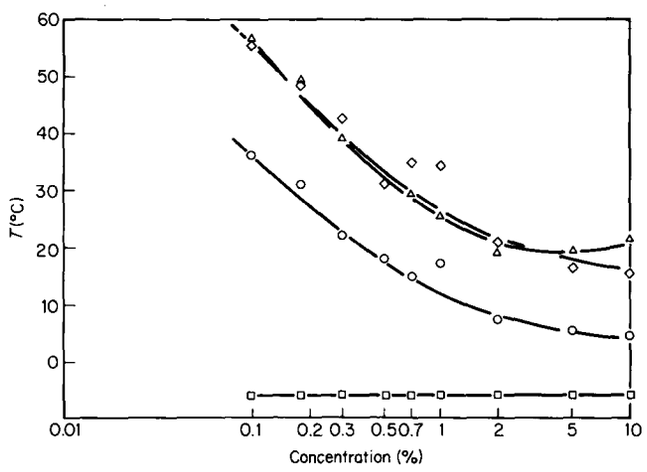

Figure 9 Effect of urea on P(SPE), $M_w = 7.1 \times 10^5$, phase behaviour. △, H_2O; ◇, 0.095 M urea; ○, 1.0 M urea; □, 2.5 M urea

that of mono- and bivalent salts. It takes more than an order of magnitude more urea to solubilize P(SPE) to the same extent as electrolytes such as $M^{\oplus\oplus}Cl_2$ (*Figures 7* and *8*). This result suggests that H-bond breaking could be an important but not a dominant factor in the solubilizing of P(SPE) by additives.

Viscometric properties

Figure 10 is a plot of the ratio of the viscosity of polymers in salt to that in H_2O, for polymers in the semidilute solution regime. The lower curve shows the expected effect of salt on the solution viscosity of a typical polyelectrolyte, e.g. poly(2-sodium acrylamido-2-methyl-propanesulphonate) [P(NaAMPS)]. The viscosity drops with increasing salt concentration because P(NaAMPS) is extended in water and is more collapsed in a brine environment. In contrast, the viscosity ratio for P(SPE) actually increases as the concentration of NaCl goes from 0% (pure H_2O) to 20% NaCl. Hence, P(SPE) acts like an 'antipolyelectrolyte'.

This effect is also seen for dilute solutions of P(SPE) with increasing levels of salt, i.e. plots of reduced viscosity (at 0.1% polymer) vs. salt concentration (*Figure 11*). As observed previously[14,15], the slope of the viscosity vs. salt curve is steepest at low concentrations of salt and then levels off at higher levels of salt. These two regimes have been interpreted as two modes of increasing chain expansion, i.e. site binding for the high slope region and atmospheric binding for the lower slope region[14].

Also at polymer concentrations < 0.5 g/dl, the reduced viscosity rises as the temperature increases. A concomitant decrease in turbidity is also noted, consistent with the previously presented phase behaviour results.

Molecular level probes

We have used several molecular level probes [i.e. static (LALLS) and dynamic (QELS)] light scattering, as well as laser Raman spectroscopy] to help understand the macroscopic properties of P(SPE) phase behaviour and viscometrics in H_2O and NaCl solutions. LALLS was used to measure changes in solvent quality with changes

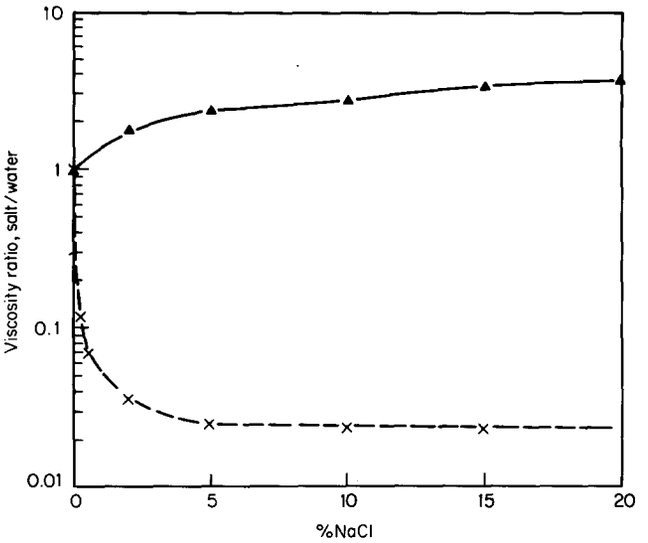

Figure 10 Effect of salt on viscosity ratio, salt/H_2O; ▲, P(SPE), $\bar{M}_w = 4.4 \times 10^5$; ×, P(NaAMPS), $\bar{M}_w = ca.\ 2.0 \times 10^6$. Polymer concentration = 1.5% (semidilute regime)

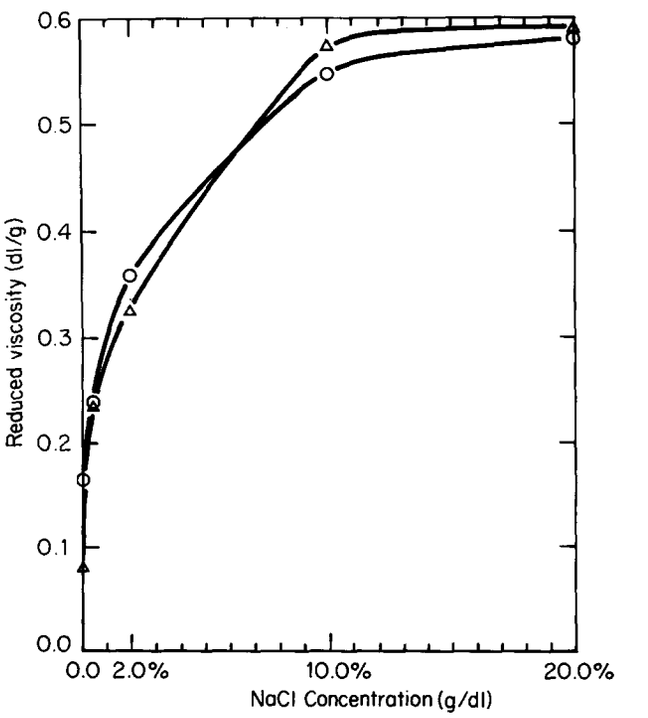

Figure 11 Reduced viscosities of P(SPE), $\bar{M}_w = 4.4 \times 10^5$, as a function of salt concentration. △, reduced viscosity of 0.1% polymer at 25°C; ○, reduced viscosity of 0.1% polymer at 40°C

in salt. QELS was employed to obtain the whole chain dimensions and dynamics, while laser Raman spectroscopy was used to examine the effects of changes in the local environment of the zwitterion functional groups. QELS and Raman spectroscopy had not previously been employed to study the properties of poly(sulphobetaines).

By static light scattering (LALLS) measurements, we studied the effects of salt concentration on solvent quality by monitoring changes in the second virial coefficient (A_2) as a function of salt concentration (*Figure 12*). Consistent with the reduced viscosity data (*Figure 11*), A_2 increases sharply with small amounts of NaCl and then levels off at higher NaCl concentrations. In other words, the solvent quality for P(SPE) increases with increasing salt concentration and the most sensitive region is the low salt region, which is presumably near the θ condition. Based upon the A_2 values, the θ state is estimated to be $\sim 0.05\%$ NaCl at 25°C.

Figure 13 shows a plot of both average hydrodynamic diameter and diffusion coefficient of a P(SPE) as a function of increasing salt concentration, as measured by QELS at 40°C. This temperature was believed to be in the 1-phase region, based upon the phase diagram for this polymer (*Figure 1*). In general (i.e. $>0.5\%$ NaCl), the hydrodynamic diameter rises with increasing salt levels, going from about 120 Å in 0.5% NaCl to about 180 Å in 20% NaCl. Moreover, the largest increases in the hydrodynamic diameter occur in the low salt regime. This is in accord with the dilute solution rheology (*Figure 11*), as expected. Of course, the diffusion coefficient response is the mirror image of the size response.

At polymer concentrations <0.5 g/dl, QELS detects the presence of small aggregates which do not contribute positively to viscosity (*Figure 11*). Thus, even though 40°C was thought to be well above the *UCST* for this P(SPE) sample, this system was not a true solution as detected by light scattering. Alternatively, the large particles detected in pure H_2O may simply reflect difficulties in obtaining a good QELS measurement in the absence of electrolytes.

Laser Raman spectroscopy—P(SPE) in H_2O and NaCl

The major features of the Raman spectrum of aqueous solutions of P(SPE) in water are attributable to water

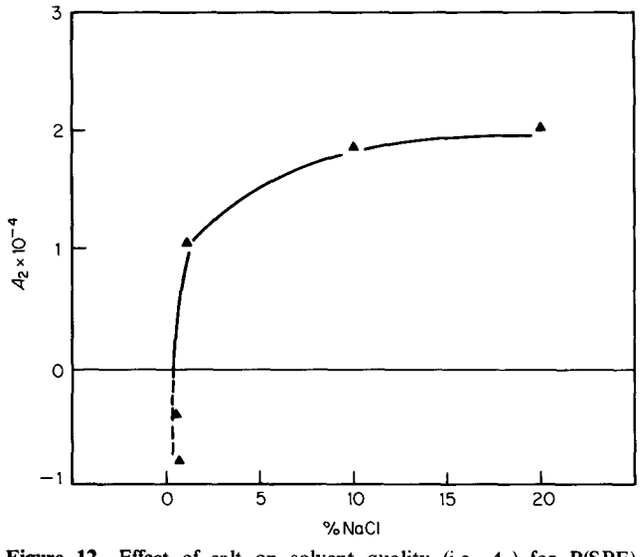

Figure 12 Effect of salt on solvent quality (i.e. A_2) for P(SPE), $\bar{M}_w = 4.4 \times 10^5$

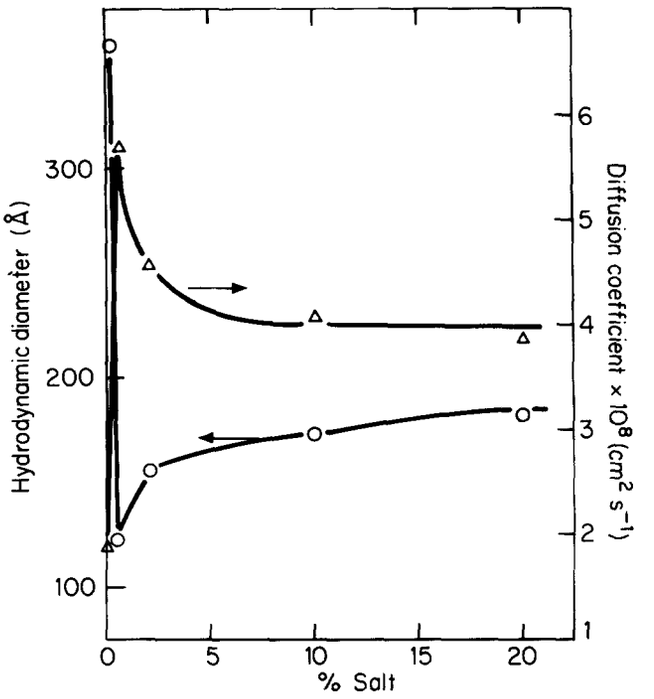

Figure 13 QELS measurements on P(SPE), $\bar{M}_w = 4.4 \times 10^5$, solution. [Polymer] = 0.1 g/dl, temperature = 40.2°C. *UCST* for this polymer was ~30°C

Table 1 Assignments of the polymer bands observed in the Raman spectra of P(SPE) aqueous solutions (H_2O bands, 1640 and 3400 cm^{-1} excluded)

Raman band (cm^{-1})	Assignment[a]
720	C–CO_2 stretch
736	
800	
824	Skeletal
922	
964	
1042	Symmetric S–O stretch
1074	Skeletal
1196	
1260	
1306	
1330	CH_2 torsion, wagging, bending
1346	
1424	
1450	
1558	$-CO_2$
ca. 1700	C=O
2848	C–H stretch
2896	C–H stretch
2942	$N^{\oplus}$–C–H stretch
2988	

[a] Refs. 27 and 28

bands (1640 cm^{-1} and ~3400 cm^{-1}) and polymer sulphonate bands (symmetric S–O stretch at 1042 cm^{-1}). Weaker bands associated with C–C stretching, C–H deformation, and $-\overset{|}{\underset{|}{N^{\oplus}}}-$C–H stretching are also observed (*Table 1*).

Changes in the spectra of P(SPE) in water and salt have been investigated using real time Raman difference spectroscopy (*Figure 14*). The major differences are in the water bands at 1640 cm^{-1} and *ca.* 3400 cm^{-1}, which shift up with salt. Of course, this solvent shift also occurs in the absence of polymer because of the known H-bond breaking effect of salts on the structure of water.

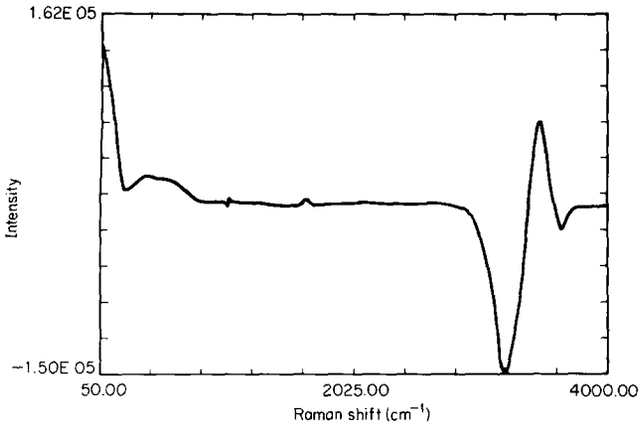

Figure 14 Difference Raman spectrum of P(SPE); (20% NaCl spectrum − 0% NaCl spectrum)

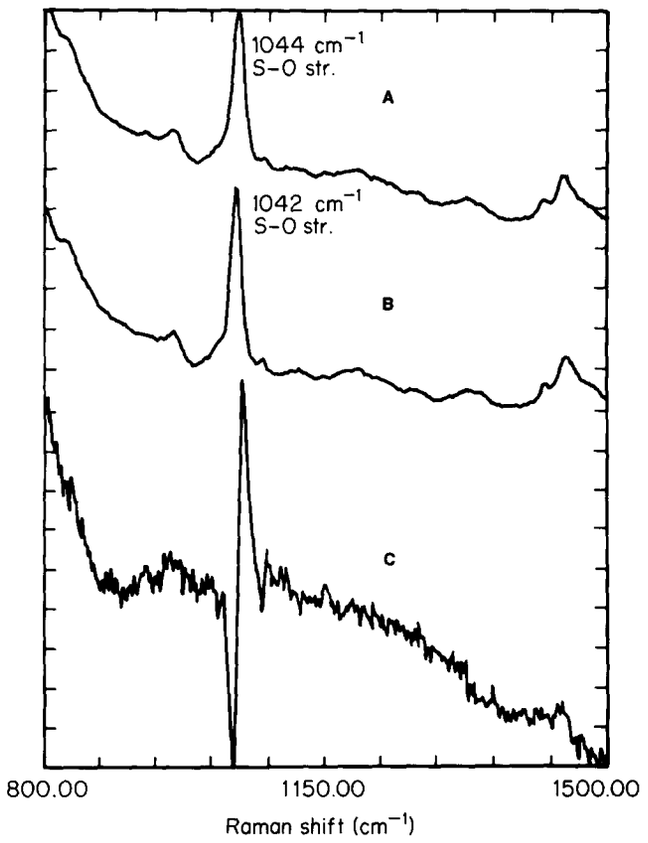

Figure 15 Expanded laser raman spectra, 800–1500 cm^{-1}. A = 1.5% P(SPE) in 20% NaCl; B = 1.5% P(SPE) in 0% NaCl; C = 20% NaCl − 0% NaCl difference spectrum

Comparing polymer bands in salt versus water, the major shift occurs in the symmetric S–O stretch at 1042 cm^{-1}. This band shifts up to 1044 cm^{-1} in salt (expanded spectrum, *Figure 15*). Thus, the S–O bond is weaker in water than in salt. Such a shift is consistent with a H-bonded $-SO_3^{\ominus}$ group in water and a more ionic (non H-bonded) $-SO_3^{\ominus}$ group in NaCl.

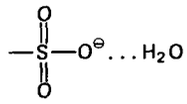

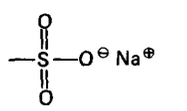

Other sulphonate monomers and polymers show a similar shift in the S–O stretch between their H_2O and NaCl spectra (*Table 2*). No other bands in the 800 to 1500 cm^{-1} region are shifted. It appears that the local environment around the $-SO_3^{\ominus}$ is changing more with addition of NaCl than the environment around the $>N^{\oplus}<$ of the zwitterion. Of course, the $>N^{\oplus}<$ region of the spectrum is partially masked by the large water shift (*Figure 14*).

Proposed model for P(SPE) in NaCl and H_2O

Our proposed schematic model to rationalize changes in the phase behaviour and solution viscometrics of P(SPE) in H_2O and NaCl is shown in *Figure 16*. In H_2O, P(SPE) has extensive intra-associations. These associations are both of the intra-chain and intra-group type. The intra-chain association results from zwitterionic and H-bonded attractions on the same chain. The intra-group associations come from intra-group ion pairs

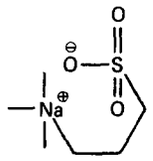

The net effect of both these types of intra-associations is to vitiate the water solubilizing effect of the ionic functionalities and render the polymer insoluble. These strong intra-associations lead to phase separation, which occurs at lower concentrations than expected. In contrast, the addition of a salt of intermediate solubilizing power like NaCl breaks up such intra-chain and intra-group associations and frees the zwitterionic functionality for aqueous solubilization of the polymer. Furthermore, the breaking of H-bonds of bound H_2O molecules to the sulphonate may yield some additional net positive charge

Table 2 Shifts observed in the S–O stretch for water soluble monomers/polymers (salt vs. water)

Polymer	Shift (cm^{-1})
Poly(SPE)	2.4
Poly(NaAMPS)	0.8
AM/SPE (70/30) copolymer	1.9
Monomers	
SPE	2.0
NaAMPS	1.4

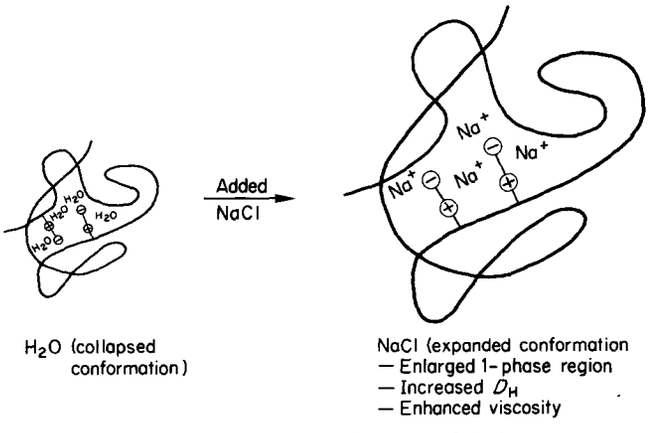

Figure 16 Proposed model P(SPE) in H_2O and NaCl

($Na^{\oplus}$) leading to increased charge repulsion. The net effect of these changes will be an expanded conformation in NaCl with an enlarged 1-phase region of solubility, increased hydrodynamic diameter, and enhanced viscosity. If NaI or NaSCN are used, the effects are likely similar in kind, except that there might be more 'action' at the $-\overset{|}{\underset{|}{N^{\oplus}}}-$ by the 'softer' $I^{\ominus}$ anion than at the sulphonate $-SO_3^{\ominus}$. Alternatively, if a 'soft' $Ag^{\oplus}$ salt were used, the 'neutralization' of the $-SO_3^{\ominus}$ might be more pronounced.

Our proposed schematic model for the effect of polymer concentration on P(SPE) phase behaviour is shown in *Figure 17*. At polymer concentrations $< 0.8\%$ at 25°C, the polymer is in a collapsed conformation and in the extreme case is in a 2-phase region. As additional polymer is added (total polymer concentration $\sim 0.8 \simeq 20\%$ at 25°C), the polymer surprisingly redissolves. (This is the 1-phase region flanked by two 2-phase regions in *Figure 1*). This solubilization occurs in the neighbourhood of the overlap concentration, C^*. We believe that this solubilization results from a shift from intra- (H-bonding and ionic) associations to a small amount of inter-associations. The presence of low levels of inter-associations results in an opening of the chain, an expansion in chain conformation, with a corresponding increase in solubility. In other words, small amounts of added polymer act like a macromolecular salt. However, when the level of inter-associations becomes too great (at polymer concentrations $> 20\%$ at 25°C) the polymer once again precipitates from solution, probably as a highly crosslinked gel.

There is some precedent for proposing dramatically different phenomena above and below C^* for ion-containing polymers. For example, Lundberg[31] has noted that the reduced viscosities of associating ionomers are greatly different above and below C^*. Above C^*, his ionomeric polymers show enhanced viscosities compared with the nonfunctional nonassociating parent polymers. Below C^*, the ionomers exhibit reduced viscosities below that of their nonfunctional counterparts. These results suggest that the ionomers have a more compact coil in dilute solution and a more highly associated state in semi-dilute solution than conventional nonfunctional polymers.

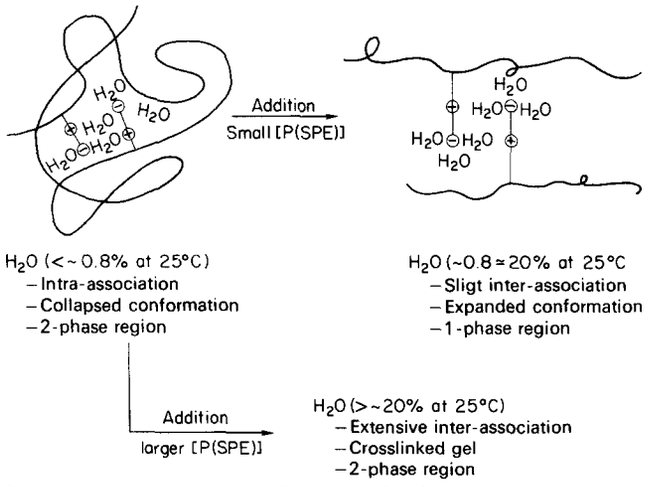

Figure 17 Proposed model for effect of polymer concentration on P(SPE) phase behaviour

SUMMARY AND CONCLUSIONS

The macroscopic phase behaviour and viscometrics of P(SPE) have been studied in water and salt solutions. P(SPE) of 4.35×10^5 M_w in water is characterized by a remarkable phase diagram. It shows both an *UCST* and what looks like an 'inverted *LCST*', or a 1-phase region flanked by two 2-phase regions. The *UCST* occurs at an order of magnitude lower polymer concentration than predicted by theory or demonstrated by experiment with conventional polymers. The *UCST* of P(SPE) is lowered by the addition of salt. Moreover, the aqueous solubility of P(SPE) is a function of polymer molecular weight, as well as the concentration and structure of the added salts. 'Soft' salt anions and cations are more effective solubilizers than 'hard' anions and cations. The viscometrics of P(SPE) exhibit an 'antipolyelectrolyte character', i.e. polymer solution viscosities which increase with increasing salt concentrations.

The macroscopic phase behaviour and viscometric properties have been studied at the molecular level using LALLS and QELS to probe the whole chain statics and dynamics and laser Raman spectroscopy to examine the local environment around the zwitterion functionalities. Static light scattering experiments indicate that the solvent quality increases with increasing salt concentration. Dynamic light scattering measurements show that the polymer diffusion coefficients decrease and the chain dimensions increase with increasing salt concentrations. Finally, laser Raman spectroscopy indicates that the local environment around the zwitterion functionality also changes with variations in salt concentration. Based upon such molecular level probes, models have been proposed to account for the P(SPE) phase behaviour and solubility. Thus, P(SPE) is depicted as a collapsed coil in water because of intra-group and intra-chain associations. The unusual phase behaviour of P(SPE) in water is rationalized in terms of a shift from intra- to inter- interactions. In turn, NaCl breaks up the intra-associations and promotes polymer solubility.

REFERENCES

1 Rice, S. A. and Nagasawa, M. 'Polyelectrolyte Solutions', Academic Press, London, New York, 1961
2 Tanford, C. 'Physical Chemistry of Macromolecules', Wiley, New York, 1961
3 Oosawa, F. 'Polyelectrolytes', Marcel Dekker, New York, 1970
4 Sèlegny, E., Mandel, M. and Strauss, U. P. (Eds.) 'Polyelectrolytes', D. Reidel, Dordrecht, Boston, 1974
5 Eisenberg, H. 'Biological Macromolecules and Polyelectrolytes in Solution', Clarendon Press, Oxford, 1976
6 Katchalsky, A., Alexandrowicz, Z. and Kedem, O. in 'Chemical Physics of Ionic Solutions', (Eds. B. E. Conway and R. G. Barradas), Wiley, New York, 1966, p. 295
7 Armstrong, R. W. and Strauss, U. P. in 'Encyclopedia of Polymer Science and Technology', Interscience, New York, 1969, p. 781
8 Katchalsky, A. *Pure Appl. Chem.* 1971, **26**, 327
9 Manning, G. S. *Ann. Rev. Phys. Chem.* 1972, **23**, 117
10 Mandel, M. *Makromol. Chem.* 1984, **123/124**, 63
11 Molyneux, P. 'Water-Soluble Synthetic Polymers: Properties and Behavior', CRC Press, Boca Raton, FL, 1984, Ch. 1
12 Finch, C. A. 'Chemistry and Technology of Water-Soluble Polymers', Plenum Press, New York, 1983
13 Hart, R. and Timmerman, D. *J. Polym. Sci.* 1958, **28**, 118
14 Salamone, J. C., Voksen, J. C., Olson, A. P. and Israel, S. C. *Polymer* 1978, **19**, 1157
15 Monroy Soto, V. M. and Galin, J. C. *Polymer* 1984, **25**, 121, 254

16 Rasching Technical Bulletin VCH-6101e-10-111/83-ME, 'Sulfopropylated Compounds', 1983
17 Kiefer, W. 'Advances in Infrared and Raman Spectroscopy', Vol. 3, (Eds. R. J. Clark and R. E. Hester), Heyden, London, 1979, Ch. 1
18 Kleintjens, L. A. and Koningsveld, R. *Macromolecules* 1984, **17**, 573
19 Solc, K. *Macromolecules* 1984, **16**, 236
20 Koningsveld, R. *Br. Polym. J.* 1975, **7**, 453
21 Koningsveld, R., Stockmeyer, W. H., Kennedy, J. W. and Kleintjens, L. A. *Macromolecules* 1974, **7**, 73
22 Flory, P. J. 'Principles of Polymer Chemistry', Cornell University Press, New York, pp. 542–548
23 Hofmeister, F. *Arch. Exptl. Pathol. Pharmakol.* 1888, **24**, 247
24 Robb, I. D. in 'Chemistry and Technology of Water Soluble Polymers', (Ed. C. A. Finch), Plenum Press, New York, 1983, Ch. 11
25 Tiddy, G., Rendall, K. and Trevettan, M. A. *Committn. Journ. Comp. Esp. Deterg.* 1984, **15**, 51
26 Pearson, R. G. 'Hard and Soft Acids and Bases', Dowden, Hutchingon and Ross, Inc., Stroudsting, PA, 1973
27 Koda, S., Nomura, H. and Nagasawa, M. *Biophys. Chem.* 1982, **15**, 65
28 Gupta, M. K. and Bansil, R. *J. Polym. Sci.* 1981, **19**, 353
29 Scherer, J. R. 'Advances in Infrared and Raman Spectroscopy', Vol. 5, (Eds. R. J. H. Clark and R. E. Hester), Heyden, London, 1980, Ch. 3
30 Lilly, T. H. in 'Water', (Ed. F. Frank), Vol. 3, Plenum, New York, 1973, Ch. 6
31 Lundberg, R. D. and Phillips, R. R. *J. Polym. Sci., Polym. Phys. Edn.* 1982, **20**, 1143